Published in IET Control Theory and Applications
Received on 7th August 2009
Revised on 3rd May 2010
doi: 10.1049/iet-cta.2009.0405

ISSN 1751-8644

Unified control for Pendubot at four equilibrium points

Z. Wang Y. Guo

Department of Electrical and Computer Engineering, Stevens Institute of Technology, Hoboken, NJ 07030, USA
E-mail: zhenwang@ucalgary.ca

Abstract: The authors consider the control of an underactuated mechanical system: Pendubot, which has four separated equilibrium points. A unified controller is proposed to stabilise the system at the four equilibrium points. Moreover, the proposed unified control can bring the underactuated link to ideal homoclinic orbits, which cannot be achieved by existing approaches. Simulation results verify the effectiveness of the proposed control.

1 Introduction

Pendubot is developed to be broadly used for education and research in non-linear control theory [1]. It is an underactuated mechanical system, and has four equilibrium points: the stable bottom position (both links are down), the unstable top position (both links are up) and two middle positions (one link is up and the other is down).

The difficulty is to design controllers to bring the non-actuated (outer) link into the vertical top position. To the best of our knowledge, there exists no continuous controller to achieve this control objective. The switching strategy has been used in [2], where two controllers are used sequentially. The first controller is called swing up control, which is based on partial feedback linearisation [2], or passivity-based control [3, 4]. The second controller is called the balancing and stabilising controller, which is typically based on linear quadratic regulator (LQR) and pole placement technique. The objective of the swing up control is to bring the outer link of Pendubot to a specific homoclinic orbit. The existing approach does not achieve, this objective, but it can bring the non-actuated link within a domain of attraction of the second controller.

The control problems at other equilibrium points were studied to obtain the periodic motion of the outer link of Pendubot using the virtual holonomic constraints approach developed in [5–7]. In [8], the convergence rate is improved by combining the virtual holonomic constraints approach with a high-gain observer design technique [9]. The existence of stable periodic motions depends on dimension-reduced zero dynamics. Moreover, the approach proposed in [8] cannot solve the primary problem discussed above since there does not exist a stable periodic motion around the unstable equilibrium point at which both links are in the top position.

In this paper, we present a unified controller to stabilise Pendubot at different equilibrium points. The manifold that involves absolute value functions is used to design the unified controller. The proposed controllers can decrease input efforts especially when the system is about to be stable. Also, the proposed controller can achieve ideal homoclinic orbits to swing the outer link up. On comparing to existing results, the proposed controller brings the outer link of Pendubot to the ideal homoclinic orbit, which cannot be achieved by all the other existing control. Moreover, unified control has the same form (with different parameters) for all equilibrium points and it may facilitate controller implementation.

The rest of the paper is organised as follows. In Section 2, the dynamics of Pendubot and the control problem is stated. The main results are presented in Section 3. The simulation results are shown in Section 4. Finally, we conclude with brief remarks in Section 5.

2 System dynamics and problem statement

Consider the two-link underactuated planar robot in Fig. 1, called Pendubot. Friction will not be considered, which is a

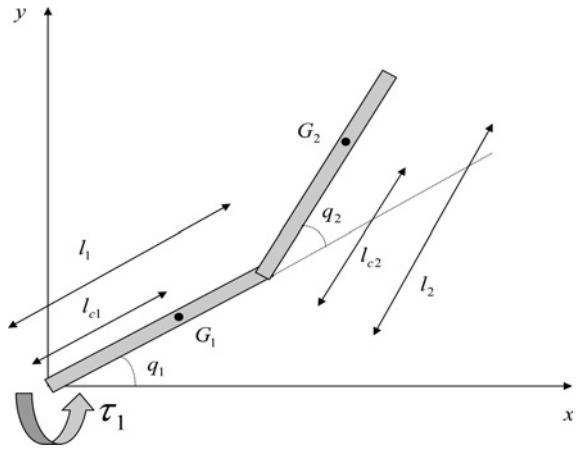

Figure 1 *Schematic diagram of Pendubot*

standard assumption on Pendubot. There are two links: Link 1 and Link 2 in Pendubot. The masses of Link 1 and Link 2 are m_1 and m_2, and their lengths are l_1 and l_2, respectively. The angle of Link 1 to the horizontal axis is denoted by q_1 and the relative angle of Link 2 to Link 1 is denoted by q_2. We denote l_{c1} as the distance of the mass centre of Link 1 and l_{c2} as the distance of the mass centre of Link 2. Moreover, I_1 and I_2 are the moments of inertia of Link 1 and Link 2, respectively.

By Euler–Lagrange formulation, the motion of Pendubot can be described as follows

$$D(q)\ddot{q} + C(q, \dot{q})\dot{q} + g(q) = \tau \tag{1}$$

where $q = [q_1\ q_2]^{\mathrm{T}}$ is the vector of generalised coordinates and $\tau = [\tau_1\ 0]^{\mathrm{T}}$ is the control input. The inertial matrix $D(q)$ is positive definite with

$$\begin{aligned} d_{11} &= \theta_1 + \theta_2 + 2\theta_3 \cos(q_2) \\ d_{12} &= d_{21} = \theta_2 + \theta_3 \cos(q_2) \\ d_{22} &= \theta_2 \end{aligned} \tag{2}$$

The elements of the Coriolis and centrifugal matrix $C(q, \dot{q})$ are

$$\begin{aligned} c_{11} &= -\theta_3 \sin(q_2)\dot{q}_2 \\ c_{12} &= -\theta_3 \sin(q_2)(\dot{q}_1 + \dot{q}_2) \\ c_{21} &= \theta_3 \sin(q_2)\dot{q}_1 \\ c_{22} &= 0 \end{aligned} \tag{3}$$

and the elements of the gravity matrix $g(q)$ are

$$\begin{aligned} g_1 &= \theta_4 g \cos(q_1) + \theta_5 g \cos(q_1 + q_2) \\ g_2 &= \theta_5 g \cos(q_1 + q_2) \end{aligned} \tag{4}$$

where

$$\begin{aligned} \theta_1 &= m_1 l_{c1}^2 + m_2 l_1^2 + I_1 \\ \theta_2 &= m_2 l_{c2}^2 + I_2 \\ \theta_3 &= m_2 l_1 l_{c2} \\ \theta_4 &= m_1 l_{c1} + m_2 l_1 \\ \theta_5 &= m_2 l_{c2} \end{aligned} \tag{5}$$

From the inertial matrix (2) and the Coriolis and centrifugal matrix (3), we calculate that

$$\dot{D}(q) - 2C(q, \dot{q}) = \theta_3 \sin q_2 (2\dot{q}_1 + \dot{q}_2) \begin{bmatrix} 0 & 1 \\ -1 & 0 \end{bmatrix} \tag{6}$$

Note that the right-hand side of (6) shows that the matrix $\dot{D}(q) - 2C(q, \dot{q})$ is skew-symmetric. In fact, this property is from obtaining the model by Newton's second law or Euler–Lagrange formulation. The details can be seen in [10].

Expanding (1), the motions of Link 1 and Link 2 of Pendubot are, respectively

$$\ddot{q}_1 = \frac{1}{d_{11}d_{22} - d_{12}^2}[d_{22}\tau_1 + F_1(q, \dot{q})] \tag{7}$$

where

$$\begin{aligned} F_1(q, \dot{q}) = (d_{12}c_{21} - d_{22}c_{11})\dot{q}_1 - d_{22}c_{12}\dot{q}_2 \\ + d_{12}g_2 - d_{22}g_1 \end{aligned} \tag{8}$$

and

$$\ddot{q}_2 = \frac{1}{d_{11}d_{22} - d_{12}^2}[-d_{12}\tau_1 + F_2(q, \dot{q})] \tag{9}$$

where

$$\begin{aligned} F_2(q, \dot{q}) = (d_{12}c_{11} - d_{11}c_{21})\dot{q}_1 + d_{12}c_{12}\dot{q}_2 \\ + d_{12}g_1 - d_{11}g_2 \end{aligned} \tag{10}$$

Pendubot (1) has four equilibrium points: $(\pi/2, 0, 0, 0)$, $(-\pi/2, 0, 0, 0)$, $(-\pi/2, 0, \pi, 0)$ and $(\pi/2, 0, -\pi, 0)$. The equilibrium point $(\pi/2, 0, 0, 0)$ is called the unstable top position, $(-\pi/2, 0, 0, 0)$ is called the stable bottom position and the remaining two equilibrium points are called unstable middle positions.

The total energy of Pendubot has the form

$$E = \frac{1}{2}\dot{q}^{\mathrm{T}} D(q)\dot{q} + \theta_4 g \sin(q_1) + \theta_5 g \sin(q_1 + q_2) \tag{11}$$

The total energies at the four equilibrium positions are,

doi: 10.1049/iet-cta.2009.0405

respectively

$$E_{\text{top}} = E\left(\frac{\pi}{2}, 0, 0, 0\right) = (\theta_4 + \theta_5)g$$

$$E_{\text{bottom}} = E\left(-\frac{\pi}{2}, 0, 0, 0\right) = (-\theta_4 - \theta_5)g$$

$$E_{\text{mid1}} = E\left(-\frac{\pi}{2}, 0, \pi, 0\right) = (-\theta_4 + \theta_5)g$$

$$E_{\text{mid2}} = E\left(\frac{\pi}{2}, 0, \pi, 0\right) = (\theta_4 - \theta_5)g$$

From the viewpoint of energy, the problem of controlling Pendubot is in general to control the total energy of Pendubot to a specific amount that is equal to the total energy at one of the equilibrium points. The difficulty of the control is to bring the non-actuated link into the unstable vertical top position. So far, there does not exist any continuous controller to stabilise Link 2 at the top position. A switching strategy has been used in [2] to solve the problem. One controller called swing up control is used to swing Link 2 up based on partial feedback linearisation [2] or passivity-based control [3, 4]. The other controller called the balancing and stabilising controller is switched to stabilise Link 2 at the top position based on LQR and pole placement technique once Link 2 enters the domain of its attraction.

Firstly, we consider Link 1. If we assume that Link 1 reaches the bottom position or the top position with zero velocity, the total energy is

$$E(q, \dot{q}) = \frac{1}{2}\theta_2\dot{q}_2^2 - \theta_4 g - \theta_5 g\cos q_2 \tag{12}$$

and

$$E(q, \dot{q}) = \frac{1}{2}\theta_2\dot{q}_2^2 + \theta_4 g + \theta_5 g\cos q_2 \tag{13}$$

respectively. Then, under these two cases we consider Link 2. If Link 2 also reaches the top position or the bottom position with zero velocity, respectively, the total energy (12) or (13) should be equal to the top energy $E_{\text{top}} = \theta_4 g + \theta_5 g$ or $E_{\text{mid1}} = (-\theta_4 + \theta_5)g$, respectively, which yields

$$\frac{1}{2}\theta_2\dot{q}_2^2 = \theta_5 g(1 + \cos q_2) \tag{14}$$

or

$$\frac{1}{2}\theta_2\dot{q}_2^2 = \theta_5 g(1 - \cos q_2) \tag{15}$$

Both (14) and (15) define homoclinic orbits whose phase portraits are shown in Figs. 2 and 3, respectively. It means that Link 2 swings clockwise or counter-clockwise until it reaches the equilibrium point $(q_2, \dot{q}_2) = (0, 0)$. Thus, swing up control should be able to bring Link 2 of Pendubot to

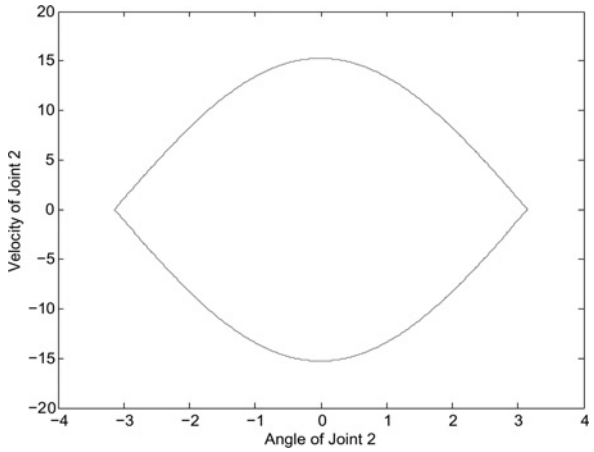

Figure 2 *Phase portrait of homoclinic orbits as* $q_1 = -\pi/2$ *and* $\dot{q}_i = 0$

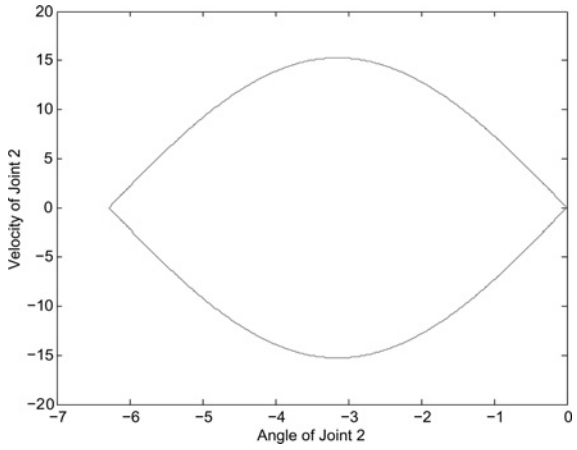

Figure 3 *Phase portrait of homoclinic orbits as* $q_1 = \pi/2$ *and* $\dot{q}_i = 0$

the homoclinic orbits (14) or (15). The existing approaches do not achieve this objective; instead, they can bring Link 2 within the domain of attraction of the balancing controller only. Moreover, the different types of controllers are used for Pendubot to stabilise at the down position or the up–down middle position and swing up for the top position or the down–up middle position.

Our objective in this paper is to design a unified controller for the Pendubot system so that only the equilibrium point in the unified controller is needed to be replaced to stabilise Pendubot at equilibrium points, $(-\pi/2, 0, 0, 0)$ and $(\pi/2, 0, -\pi, 0)$, or swing up at equilibrium points, $(\pi/2, 0, 0, 0)$ and $(-\pi/2, 0, \pi, 0)$, such that the motion of Link 2 reaches the homoclinic orbits defined in (14) or (15).

3 Unified control of Pendubot at different equilibrium points

Let q_{ie}, $i = 1, 2$, be one of the equilibrium points described in the previous section. After using the following

transformation

$$\begin{aligned} x_1 &= q_1 - q_{1e} \\ x_2 &= \dot{q}_1 \\ x_3 &= q_2 - q_{2e} \\ x_4 &= \dot{q}_2 \end{aligned} \tag{16}$$

Pendubot (1) can be transformed into the following error model

$$\begin{aligned} \dot{x}_1 &= x_2 \\ \dot{x}_2 &= \frac{1}{d_{11}d_{22} - d_{12}^2}(d_{22}\tau_1 + F_1(q, \dot{q})) \\ \dot{x}_3 &= x_4 \\ \dot{x}_4 &= \frac{1}{d_{11}d_{22} - d_{12}^2}(-d_{12}\tau_1 + F_2(q, \dot{q})) \end{aligned} \tag{17}$$

Since Pendubot is underactuated, which means that the number of control is less than the degree of freedom, it is very hard to control it. Most control approaches for underactuated systems are trying to use some constraints [11–13] to reduce the number of degrees of freedom on purpose. These approaches can be thought of as a variation of partial feedback linearisation. However, how to choose the constraint for the control design is a difficult problem. Backstepping control [14] is an effective method to control an underactuated system. Unfortunately, it only works for systems with a special structure. For Pendubot, backstepping does not work for swing up control. In [15], sliding mode control was used for a class of underactuated systems. The difficulty of this method is how to choose a stable manifold. In this section, we try to eliminate these problems. A manifold described by the absolute value function is used to swing up Link 2 and to bring Link 1 to the desired position simultaneously.

Let

$$\begin{aligned} S(x) = {} & w_1|s_1x_1 + x_2| + w_2|x_2 + s_2x_4| + w_3|x_2| \\ & + w_4|x_2 + x_3 + s_2x_4| + \frac{1}{2}k_1x_1^2 + \frac{1}{2}k_2x_3^2 \end{aligned} \tag{18}$$

where $w_i > 0$, $i = 1, 2, 3, 4$, are weighting coefficients and $s_i > 0$, $k_i > 0$, $i = 1, 2$, are positive constants. If there exists a controller to squeeze system (17) to the manifold $S = 0$, from (18) we can obtain that x_1 and x_2 converge simultaneously. The problem is how to find such a controller to push a system to this manifold $S = 0$. We use sliding mode control to design such a controller.

Theorem 1: For system (17), if non-zero weighting coefficients $w_i > 0$, $i = 1, 2, 3, 4$, satisfy

$$\begin{aligned} w_1 &\neq w_3 \\ w_2 &\neq w_4 \end{aligned} \tag{19}$$

$$0 < s_2 < \frac{\theta_2}{\theta_2 + \theta_3} \tag{20}$$

$$\begin{aligned} & \frac{\min\{w_1, w_3, |w_1 - w_3|, |w_1 + w_3|\}}{\max\{w_2, w_4, |w_2 - w_4|, |w_2 + w_4|\}} \\ & > \max\left\{\left|\left(1 - \frac{\theta_3}{\theta_2}\right)s_2 - 1\right|, \left|\left(1 + \frac{\theta_3}{\theta_2}\right)s_2 - 1\right|\right\} \end{aligned} \tag{21}$$

the solution of the closed-loop system with the following control law

$$\tau_1 = \begin{cases} 0 & \text{if } r_1 = r_2 = r_3 = r_4 = 0 \\ \dfrac{M(x)}{N(x)} & \text{elsewhere} \end{cases} \tag{22}$$

where $r_1 = \text{sign}(s_1x_1 + x_2)$, $r_3 = \text{sign}(x_2)$, $r_2 = \text{sign}(x_2 + s_2x_4)$ and $r_4 = \text{sign}(x_2 + x_3 + s_2x_4)$ in which $\text{sign}(x)$ is signum function of a real number x defined as follows

$$\text{sign}(x) = \begin{cases} -1 & \text{if } x < 0 \\ 0 & \text{if } x = 0 \\ 1 & \text{if } x > 0 \end{cases} \tag{23}$$

and

$$\begin{aligned} M(x) = {} & -(\rho S + k_1x_1x_2 + k_2x_3x_4 + w_1r_1s_1x_2 + w_4r_4x_4) \\ & \times (d_{11}d_{22} - d_{12}^2) - (w_1r_1 + w_3r_3 + w_2r_2 + w_4r_4)F_1 \\ & - (s_2w_2r_2 + s_2w_4r_4)F_2 \end{aligned} \tag{24}$$

$$\begin{aligned} N(x) = {} & (w_1r_1 + w_3r_3 + w_2r_2 + w_4r_4)d_{22} \\ & - (s_2w_2r_2 + s_2w_4r_4)d_{12} \end{aligned} \tag{25}$$

converges to a point or an invariant set M, which is given by homoclinic orbits (14) or (15).

Proof: Firstly, we prove that if s_2 and the weighting coefficients w_i, $i = 1, 2, 3, 4$, satisfy the conditions from (19) to (21), then the following inequality holds

$$N(x) \neq 0, \quad \text{as} \quad (r_1, r_2, r_3, r_4) \neq 0 \tag{26}$$

Substituting d_{12} and d_{22} into $N(x)$ gives

$$\begin{aligned} N(x) = {} & (w_1r_1 + w_3r_3 + (1 - s_2)(w_2r_2 + w_4r_4))\theta_2 \\ & - s_2(w_2r_2 + w_4r_4)\theta_3\cos(q_2) \end{aligned} \tag{27}$$

Suppose that $(r_1, r_2, r_3, r_4) \neq \mathbf{0}$. There are two cases: $w_2r_2 + w_4r_4 = 0$ and $w_2r_2 + w_4r_4 \neq 0$.

Case 1: $w_2r_2 + w_4r_4 = 0$. Since $w_2 \neq w_4$, $w_2r_2 + w_4r_4 = 0$ yields $r_2 = r_4 = 0$. Thus $N(x) = w_1r_1 + w_3r_3$. If $N(x) = 0$,

doi: 10.1049/iet-cta.2009.0405

we have $w_1r_1 + w_3r_3 = 0$. Since $w_1 \neq w_3$, $w_1r_1 + w_3r_3 = 0$ yields $r_1 = r_3 = 0$. This is contradictory to the assumption $(r_1, r_2, r_3, r_4) \neq \mathbf{0}$. So $N(x)$ cannot be zero.

Case 2: $w_2r_2 + w_4r_4 \neq 0$. When $r_1 = r_3 = 0$, $N(x) = (1 - s_2)(w_2r_2 + w_4r_4)\theta_2 - s_2(w_2r_2 + w_4r_4)\theta_3\cos(q_2)$. From (20) and $|\cos(q_2)| \leq 1$, we obtain $N(x) \neq 0$. Suppose that r_1 and r_3 are not equal to zero at the same time. If $N(x) = 0$, we have $\cos(q_2) = X + 1 - s_2/s_2 \cdot \theta_2/\theta_3$, where $X = w_1r_1 + w_3r_3/w_2r_2 + w_4r_4$. Since $|\cos(x_3)| \leq 1$ and $s_2 > 0$, X should be in the interval $\left[(1 - (\theta_3/\theta_2))s_2 - 1, (1 + (\theta_3/\theta_2))s_2 - 1\right]$. However, (21) yields

$$|X| > \max\left\{\left|\left(1 - \frac{\theta_3}{\theta_2}\right)s_2 - 1\right|, \left|\left(1 + \frac{\theta_3}{\theta_2}\right)s_2 - 1\right|\right\}$$

when r_1 and r_3 are not equal to zero at the same time. This shows that X is outside of the interval $[(1 - (\theta_3/\theta_2))s_2 - 1, (1 + (\theta_3/\theta_2))s_2 - 1]$. Thus, $N(x) \neq 0$.

Now we discuss the stability of the closed-loop systems. We choose $P = (1/2)S^2$ as a Lyapunov function candidate. Taking the derivative of P along the solutions of (17) gives

$$\begin{aligned}\dot{P} &= S\dot{S}\\ &= S(w_1r_1(s_1x_2 + \dot{x}_2) + w_2r_2(\dot{x}_2 + s_2\dot{x}_4)\\ &\quad + w_3r_3\dot{x}_2 + w_4r_4(\dot{x}_2 + x_3 + s_2\dot{x}_4))\\ &= S((w_1r_1 + w_3r_3 + w_2r_2 + w_4r_4)\dot{x}_2\\ &\quad + s_2(w_2r_2 + w_4r_4)\dot{x}_4\\ &\quad + w_1r_1s_1x_2 + w_4r_4x_4 + x_1x_2 + x_3x_4)\end{aligned} \tag{28}$$

Substituting (17) and (22) into (28) gives

$$\dot{P} = -\rho S^2 \tag{29}$$

which guarantees that S goes to zero. From the definition of S in (18), $S = 0$ if and only if $x_1 = x_2 = x_3 = x_4 = 0$. From the Lyapunov theorem ([9] Theorem 4.1), the closed-loop system (17) and (22) is stable. □

Remark 1: Note that the controller (22) is discontinuous since the signum function is used. The magnitude of the controller becomes small when the system is about to be stable. Like any sliding mode control, chattering may occur.

Remark 2: The approach of designing the controller (22) can be an effective method for general underactuated control systems. This is because the manifold involves the absolute value functions so that the multiple objectives can be considered simultaneously. To construct a manifold that involves absolute value functions is much easier than to figure out the constraints needed in other methods such as the virtual constraints method or the immersion and invariance method [11, 13].

Since the term $|x_2 + s_2x_4|$ in (18), a virtual constraint between x_2 and x_4, which are velocity errors of Joints 1 and 2, is forced by the control (22) in Theorem 1 that would affect the performance, especially for swing up control. For a special case where $\theta_2 > \theta_3$, this constraint is not needed any more. By setting a new manifold for the system (17) with $\theta_2 > \theta_3$

$$\begin{aligned}S(x) &= w_1|s_1x_1 + x_2| + w_2|s_2x_3 + x_4|\\ &\quad + w_3|x_2| + w_4|x_4| + \frac{1}{2}k_1x_1^2 + \frac{1}{2}k_2x_3^2\end{aligned} \tag{30}$$

we have the following theorem:

Theorem 2: For the system (17) with $\theta_2 > \theta_3$, if weighting coefficients w_i, $i = 1, 2, 3, 4$, satisfy

$$\begin{aligned}&w_1 \neq w_3\\ &w_2 \neq w_4\\ &\frac{\min\{w_1, w_3, |w_1 - w_3|, |w_1 + w_3|\}}{\max\{w_2, w_4, |w_2 - w_4|, |w_2 + w_4|\}}\\ &\quad > \max\left\{\left|1 - \frac{\theta_3}{\theta_2}\right|, \left|1 + \frac{\theta_3}{\theta_2}\right|\right\}\end{aligned} \tag{31}$$

the solution of the closed-loop system with the following control law converges to a point or an invariant set M, which is given by homoclinic orbits (14) or (15).

$$u = \begin{cases} 0 & \text{if } r_1 = r_2 = r_3 = r_4 = 0\\ \dfrac{M(x)}{N(x)} & \text{elsewhere}\end{cases} \tag{32}$$

where

$$\begin{aligned}M(x) &= -(\rho S + k_1x_1x_2 + k_2x_3x_4 + w_1r_1s_1x_2 + w_2r_2s_2x_4)\\ &\quad \times (d_{11}d_{22} - d_{12}^2) - (w_1r_1 + w_3r_3)F_1\\ &\quad - (w_2r_2 + w_4r_4)F_2\end{aligned} \tag{33}$$

$$N(x) = (w_1r_1 + w_3r_3)d_{22} - (w_2r_2 + w_4r_4)d_{12} \tag{34}$$

and $r_1 = \text{sign}(s_1x_1 + x_2)$, $r_3 = \text{sign}(x_2)$, $r_2 = \text{sign}(s_2x_3 + x_4)$ and $r_4 = \text{sign}(x_4)$.

Proof: Firstly, we prove that if the weighting coefficients w_i, $i = 1, 2, 3, 4$, satisfy the conditions in (31), then

$$N(x) \neq 0, \quad \text{as} \quad (r_1, r_2, r_3, r_4) \neq 0 \tag{35}$$

Substituting d_{12} and d_{22} into $N(x)$ gives

$$\begin{aligned}N(x) &= (w_1r_1 + w_3r_3 - w_2r_2 - w_4r_4)\theta_2\\ &\quad - (w_2r_2 + w_4r_4)\theta_3\cos(q_2)\end{aligned} \tag{36}$$

Suppose that $(r_1, r_2, r_3, r_4) \neq \mathbf{0}$. There are two cases: $w_2r_2 + w_4r_4 = 0$ and $w_2r_2 + w_4r_4 \neq 0$.

Case 1: $w_2r_2 + w_4r_4 = 0$. Since $w_2 \neq w_4$, $w_2r_2 + w_4r_4 = 0$ yields $r_2 = r_4 = 0$. Thus $N(x) = w_1r_1 + w_3r_3$. If $N(x) = 0$, we have $w_1r_1 + w_3r_3 = 0$. Since $w_1 \neq w_3$, $w_1r_1 + w_3r_3 = 0$ yields $r_1 = r_3 = 0$. This is contradictory to the assumption $(r_1, r_2, r_3, r_4) \neq \mathbf{0}$. So $N(x)$ cannot be zero.

Case 2: $w_2r_2 + w_4r_4 \neq 0$. When $r_1 = r_3 = 0$, $N(x) = -(w_2r_2 + w_4r_4)\theta_2 - (w_2r_2 + w_4r_4)\theta_3 \cos(q_2)$. From $\theta_2 < \theta_3$ and $|\cos(q_2)| \leq 1$, we obtain $N(x) \neq 0$. Suppose that r_1 and r_3 are not equal to zero at the same time. If $N(x) = 0$, we have $\cos(q_2) = (X - 1)(\theta_2/\theta_3)$, where $X = w_1r_1 + w_3r_3/w_2r_2 + w_4r_4$. Since $|\cos(q_2)| \leq 1$, X should be in the interval $[1 - (\theta_3/\theta_2), 1 + (\theta_3/\theta_2)]$. However, (31) yields

$$|X| > \max\left\{\left|1 - \frac{\theta_3}{\theta_2}\right|, \left|1 + \frac{\theta_3}{\theta_2}\right|\right\}$$

when r_1 and r_3 are not equal to zero at the same time. This shows that X is outside the interval $[1 - (\theta_3/\theta_2), 1 + (\theta_3/\theta_2)]$. Thus, $N(x) \neq 0$. The rest of the proof is similar to the proof of Theorem 1. □

Remark 3: Note that $\theta_2 > \theta_3$ if $l_{c2} > l_1$, where l_{c2} is the distance of the mass centre of Link 2 and l_1 is the length of Link 1.

4 Simulation

In order to simulate using Matlab Simulink, we choose the system parameters $\theta_1 = 0.0308$, $\theta_2 = 0.0106$, $\theta_3 = 0.0095$, $\theta_4 = 0.2086$ and $\theta_5 = 0.0630$, which are used in [3, 4]. Since $\theta_2 > \theta_3$, Theorem 1 can be used to design controllers.

We choose $w_1 = 10$, $w_2 = 1$, $w_3 = 5$, $w_4 = 2$ and $k_1 = 2$, $k_2 = 10$ as the weighting coefficients of S defined by (30), which satisfy the conditions (31).

We consider Case 1: the equilibrium point is $q_1 = \pi/2$ and $q_2 = -\pi$. We choose $\rho = 1.4$, $s_1 = .05$ and $s_2 = 5$. Initial conditions are $q_1 = -\pi/2$, $\dot{q}_1 = 0$ and $q_2 = 0$, $\dot{q}_2 = 0$. Figs. 4 and 5 show that the angles of Joints 1 and 2 converge to the equilibrium point $q_1 = \pi/2$ and $q_2 = -\pi$ although small oscillation occurs. The small figure in the right-up corner of Fig. 5 shows the angles of Joint 2 in the last 5 s, from which we can tell that the trend of the curve is still going down. Our proposed controller (22) stabilises Pendubot at the unstable equilibrium point $q_1 = \pi/2$ and $q_2 = -\pi$. From Fig. 6 the control forces are reasonably small. Fig. 7 shows that S approaches zero by applying control (22).

Now, consider Case 2: the equilibrium point $q_1 = \pi/2$ and $q_2 = 0$. From the description in Section 2, we know that Pendubot will be involved in the homoclinic orbit described by (15). In this case, we use our proposed

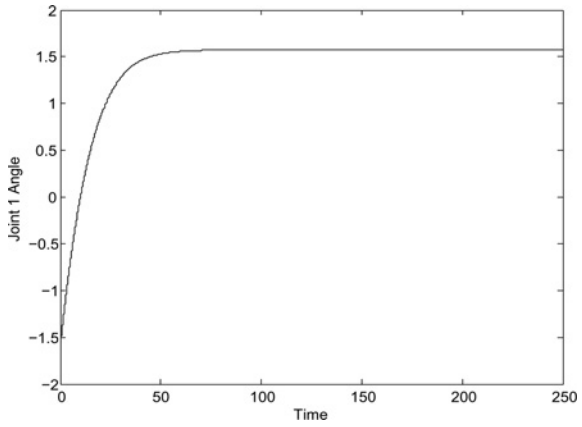

Figure 4 *Angle response of Joint 1 at unstable equilibrium points $q_1 = \pi/2$ and $q_2 = -\pi$ with control parameter $\rho = 1.4$*

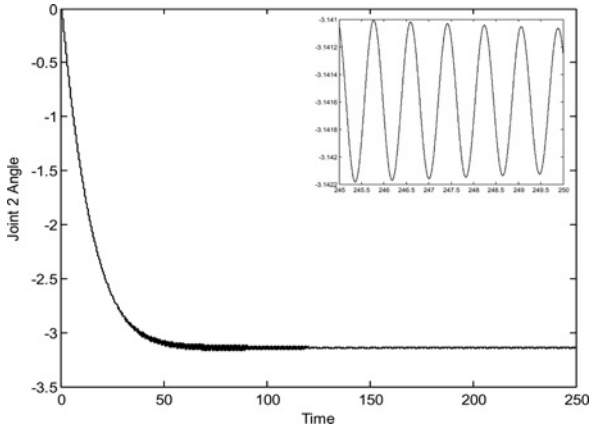

Figure 5 *Angle response of Joint 2 at unstable equilibrium points $q_1 = \pi/2$ and $q_2 = -\pi$ with control parameter $\rho = 1.4$*

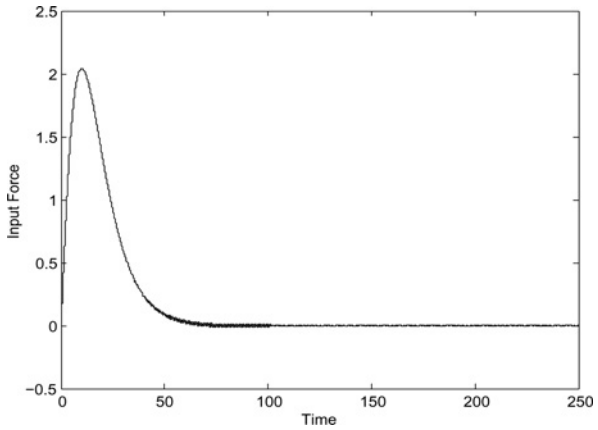

Figure 6 *Input force at unstable equilibrium points $q_1 = \pi/2$ and $q_2 = -\pi$ with control parameter $\rho = 1.4$*

doi: 10.1049/iet-cta.2009.0405

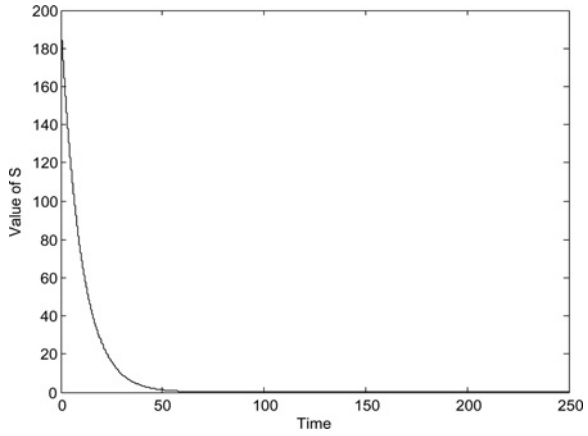

Figure 7 *Value of manifold S defined in (18)*

controller (22) but with different control parameters $\rho = 25$, $s_1 = 5$ and $s_2 = 5$. Figs. 8 and 9 show that the angle of Joint 1 converges to $\pi/2$ while the angle of Joint 2 becomes a motion that gets close to the desired homoclinic orbit given by (15) gradually. However, Fig. 10 shows that the desired

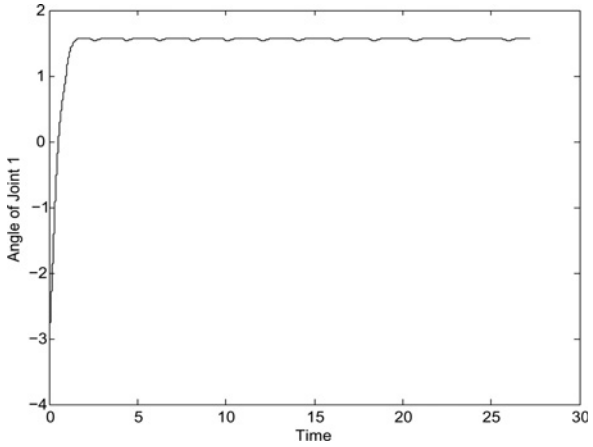

Figure 8 *Angle response of Joint 1 at unstable equilibrium points $q_1 = \pi/2$ and $q_2 = 0$ with control parameter $\rho = 2.8$*

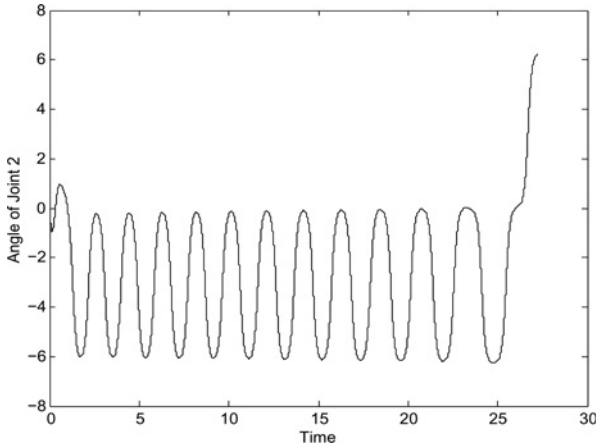

Figure 9 *Angle response of Joint 2 at unstable equilibrium points $q_1 = \pi/2$ and $q_2 = 0$ with control parameter $\rho = 2.8$*

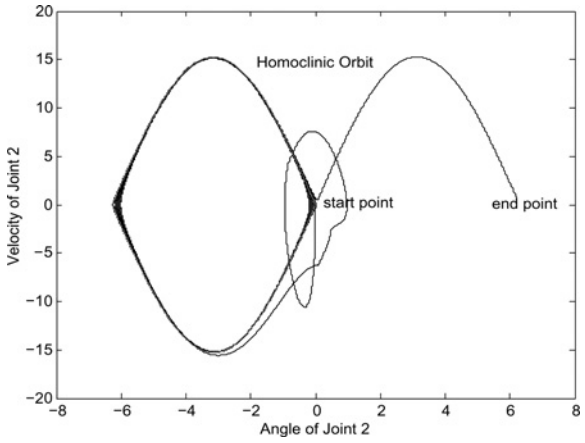

Figure 10 *Phase portrait of Joint 2 at unstable equilibrium points $q_1 = \pi/2$ and $q_2 = 0$ with control parameter $\rho = 2.8$*

homoclinic orbit is not stable. Once the motion of Joint 2 reaches the homoclinic orbit, the controller will repel the motion of Link 2 away from the desired homoclinic orbit. Fig. 11 shows the control forces.

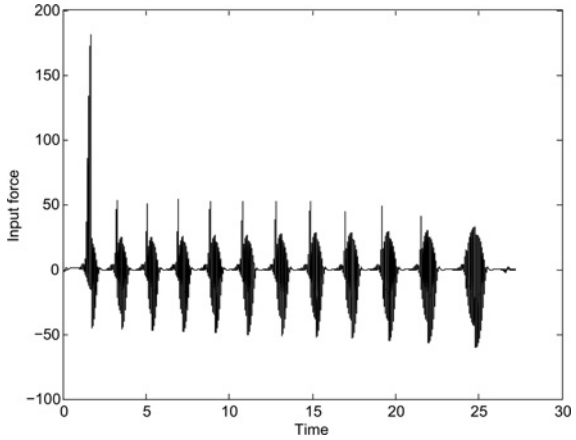

Figure 11 *Input force at unstable equilibrium points $q_1 = \pi/2$ and $q_2 = 0$ with control parameter $\rho = 2.8$*

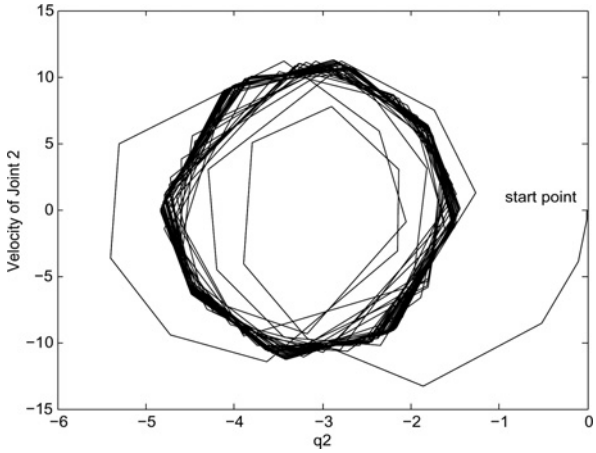

Figure 12 *Phase portrait of homoclinic orbits*

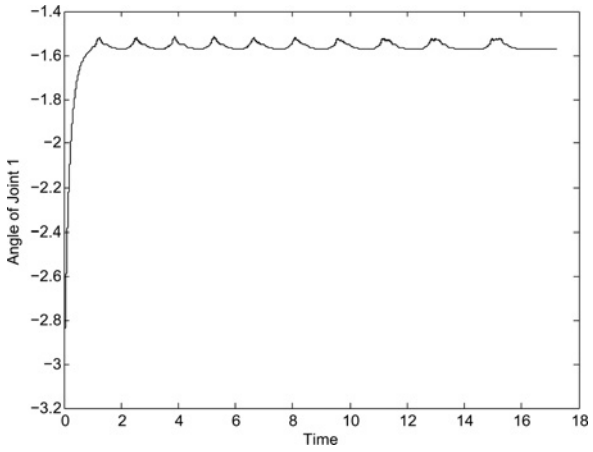

Figure 13 *Angle response of Joint 1 at unstable equilibrium points $q_1 = -\pi/2$ and $q_2 = \pi$ with control parameter $\rho = 90$*

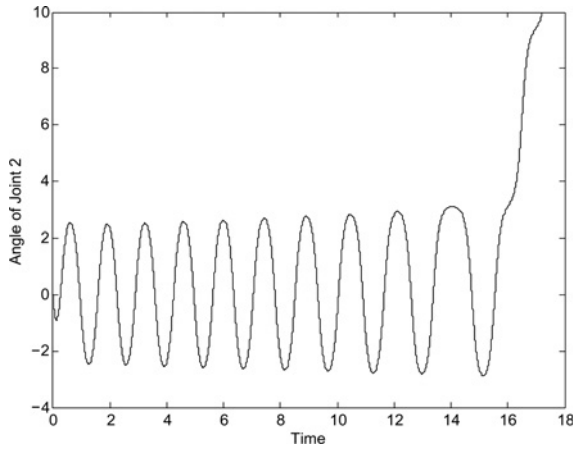

Figure 14 *Angle response of Joint 2 at unstable equilibrium points $q_1 = -\pi/2$ and $q_2 = \pi$ with control parameter $\rho = 90$*

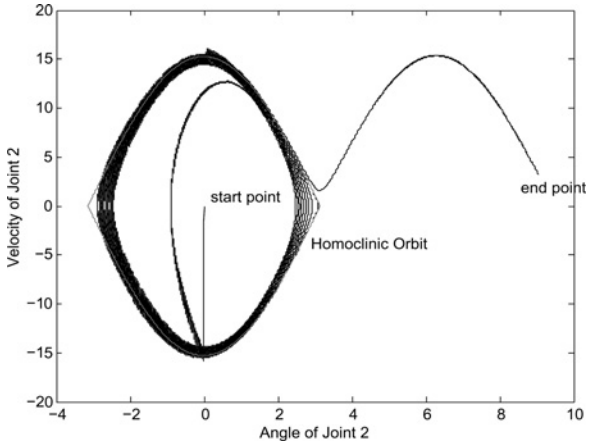

Figure 15 *Phase portrait of Joint 2 at unstable equilibrium points $q_1 = -\pi/2$ and $q_2 = \pi$ with control parameter $\rho = 90$*

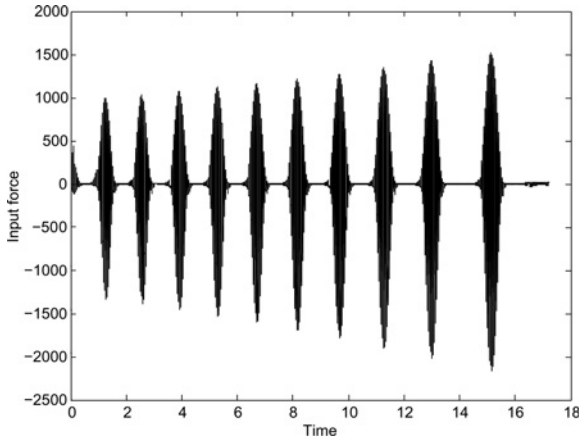

Figure 16 *Input force at unstable equilibrium points $-q_1 = \pi/2$ and $q_2 = \pi$ with control parameter $\rho = 90$*

The phase portrait of q_2 and $\dot{q}_2$ using the approach developed in [3, 4] is shown in Fig. 12. Comparing it to Fig. 3, we can see that the swing control developed in [3, 4] does not bring the system to the desired homoclinic orbit defined in (15).

Case 3: the equilibrium point $q_1 = -\pi/2$ and $q_2 = 0$. The control parameter is chosen to be $\rho = 190$, $s_1 = 5$ and $s_2 = 5$. Figs. 13 and 14 show that similar motion has been obtained by our proposed controller and q_1 goes to $-\pi/2$. The homoclinic orbit described by (14) is achieved but not stable in Fig. 15. Fig. 16 shows that the control forces needed in Case 3 are much greater than that in Case 2.

5 Conclusion

In this paper, we consider the control of an underactuated mechanical system: Pendubot, which has four separated equilibrium points. A unified controller is proposed so that only the known equilibrium point information is needed to stabilise the Pendulum at the four different equilibrium points. Moreover, our proposed unified control can bring the underactuated link to ideal homoclinic orbits that cannot be achieved by existing approaches. Simulation results validate the effectiveness of the proposed approach. The method proposed in this paper may be applied to other underactuated control systems.

6 Acknowledgments

This work was supported in part by the National Science Foundation under Grants CMMI 0825613 and DUE 0837584. We would also like to thank the anonymous reviewers for their constructive comments.

7 References

[1] SPONG M.W., BLOCK D.J.: 'The pendubot: a mechatronic system for control research and education'. Proc. 35th

doi: 10.1049/iet-cta.2009.0405

IEEE Conf. on Decision and Control, New Orleans, USA, 1995, pp. 555–557

[2] BLOCK D.J.: 'Mechanical design and control of the Pendubo'. Master Thesis, University of Illinois, Urbana-Champaign, IL, USA, 1996

[3] FANTONI I., LOZANO R., SPONG M.W.: 'Passivity based control of the Pendubot'. Proc. American Control Conf., San Diego, CA, USA, 1999, pp. 268–272

[4] FANTONI I., LOZANO R., SPONG M.W.: 'Energy based control of the Pendubot', *IEEE Trans. Autom. Control*, 2000, **45**, (4), pp. 725–729

[5] SHIRIAEV A.S., PERRAM J.W., ROBERTSSON A., SANDBERG A.: 'Periodic motion planning for virtually constrained Euler-Lagrange systems', *Syst. Control Lett.*, 2006, **55**, (11), pp. 900–907

[6] SHIRIAEV A.S., PERRAM J.W., CANUDAS-DE-WIT C.: 'Constructive tool for orbital stabilization of underactuated nonlinear systems: virtual constraints approach', *IEEE Trans. Autom. Control*, 2005, **50**, (8), pp. 1164–1176

[7] SHIRIAEV A.S., FREIDOVICH L.B., ROBERTSSON A., JOHANSSON R., SANDBERG A.: 'Virtual-holonomic-constraints-based design of stable oscillations of Furuta pendulum: theory and experiments', *IEEE Trans. Robot.*, 2007, **23**, (4), pp. 827–832

[8] FREIDOVICH L., ROBERTSSON A., SHIRIAEV A., JOHANSSON R.: 'Periodic motions of the Pendubot via virtual holomonic constraints: theory and experiments', *Automatica*, 2008, **44**, (3), pp. 785–791

[9] KHALIL H.K.: 'Nonlinear systems' (Prentice-Hall, New Jersey, 2002, 3rd edn.)

[10] SPONG M., VIDYASAGAR M.: 'Robot dynamics and control' (John Wiley, New York, 1998, 2nd edn.)

[11] ACOSTA J.A., ORTEGA R., ASTOLFI A., SARRAS I.: 'A constructive solution for stabilization via immersion and invariance: the cart and pendulum system', *Automatica*, 2008, **44**, (9), pp. 2352–2357

[12] ASTOLFI A., KARAGIANNIS D., ORTEGA R.: 'Nonlinear and adaptive control design and applications' (Springer-Verlag, London, 2007)

[13] ASTOLFI A., ORTEGA R.: 'Immersion and invariance: a new tool for stabilization and adaptive control of nonlinear systems', *IEEE Trans. Autom. Control*, 2003, **48**, (4), pp. 590–606

[14] ANEKE N.P.I., NIJMEIJER H., DE JAGER A.G.: 'Trajectory tracking by cascaded backstepping control for a second-order nonholonomic mechanical system', in ISIDORI A., LAGARRIGUE F., RESPONDEK W. (EDS.): 'Nonlinear control in the year 2000', (*LNCS*, **258**), (Springer-Verlag, Heidelberg, 2001), pp. 35–47

[15] XU R., OZGUNER U.: 'Sliding mode control of a class of underactuated systems', *Automatica*, 2008, **44**, (1), pp. 233–241